

Productions of second Kaluza-Klein gauge bosons in the minimal universal extra dimension model at LHC

Shigeki Matsumoto^{a,1}, Joe Sato^{b,2}, Masato Senami^{c,3},
and Masato Yamanaka^{b,4}

^a*Department of Physics, University of Toyama, Toyama 930-8555, Japan*

^b*Department of Physics, Saitama University, Shimo-okubo, Sakura-ku, Saitama,
338-8570, Japan*

^c*Department of Micro Engineering, Kyoto University, Kyoto 606-8501, Japan*

This author was in ICRR, Univ. of Tokyo, when this work started.

Abstract

We calculate the production rates of the second Kaluza-Klein (KK) photon $\gamma^{(2)}$ and Z boson $Z^{(2)}$ at the LHC including all significant processes in the minimal universal extra dimension model. For discrimination of the minimal universal extra dimension model from other TeV scale models in the hadron collider experiment, $\gamma^{(2)}$ and $Z^{(2)}$ play a crucial role. In order to discuss the discrimination and calculate their production rates, we derive effective Lagrangian containing KK number violating operators. We show that KK number violating processes are extremely important for the compactification scale larger than 800 GeV. We find that, with an integrated luminosity of 100 fb⁻¹, the number of produced $\gamma^{(2)}$ and $Z^{(2)}$ are estimated as 10⁶ - 10² for the compactification scale between 400 GeV and 2000 GeV.

¹smatsu@sci.u-toyama.ac.jp

²joe@phy.saitama-u.ac.jp

³senami@me.kyoto-u.ac.jp

⁴masa@krishna.phy.saitama-u.ac.jp

1 Introduction

Theoretical arguments in particle physics and cosmological observations conclude that the Standard Model (SM) is not the theory of everything but is rather the effective theory describing physics below $\mathcal{O}(100)$ GeV. Many models beyond the SM have been proposed, and the Universal Extra Dimension (UED) models [1] are some of the attractive candidates for new physics at TeV scale¹. In the UED models, all SM fields can propagate into compactified extra dimensions, and hence they are accompanied by the tower of Kaluza-Klein (KK) particles. They can give plausible explanations for the existence of dark matter [3], the number of fermion generations [4], SM neutrino masses which are embedded in extended models [5], and so on. Among various UED models, the simplest and the most popular one is called the Minimal UED (MUED) model. The MUED model is defined on the five dimensional space-time, where the extra dimension is compactified on an S^1/Z_2 orbifold. In the MUED model, only two parameters are newly introduced to the SM. One is the compactification scale of the extra dimension $1/R$, the inverse of the radius of S^1 circle, and the other is the cutoff scale of the MUED model Λ . In order to satisfy terrestrial experiments, $1/R$ must be larger than 400 GeV [1, 6], while the calculation of the relic abundance of the lightest KK particle (LKP) suggests that the abundance of the dark matter is explained for $500 \text{ GeV} \lesssim 1/R \lesssim 1500 \text{ GeV}$ [7]. As indicated from these results, the MUED model would be discovered and studied at the Large Hadron Collider (LHC).

The confirmation of the MUED model (in general, UED models) at collider experiments requires the discovery of KK particles. Though the LHC can produce KK particles, it is difficult to confirm that they are indeed the KK particles, because new particles predicted in various TeV scale models give quite similar signatures to each other. Therefore it is very important to understand how they can be identified as KK particles. In this article, we discuss the discrimination of the MUED model from other TeV scale models.

In Ref. [8], an excellent idea to discriminate the MUED model from other TeV scale models has been proposed. The essence of the discrimination is the discovery of the second KK particles. The signals of the first KK particles are quite similar to those of new particles in other models. However, the discovery of the second KK particles strongly suggests the existence of the MUED model, since their masses are peculiarly almost equal to $2/R$, and the value of $1/R$ is expected by the masses of the “first KK” particles. In particular, the second KK photon $\gamma^{(2)}$ and Z boson $Z^{(2)}$ play an important role for the search of the second KK particles. They are able to

¹UED models are motivated by the TeV scale extra dimension theory [2].

decay into two charged leptons. It is possible to reconstruct the masses of $\gamma^{(2)}$ and $Z^{(2)}$ clearly from the charged dileptons emitted by them. Connecting their masses and those of the first KK particles, we can confirm the realization of the MUED model.

Hence, $\gamma^{(2)}$ and $Z^{(2)}$ are the key ingredients to discriminate the MUED model from other TeV scale models. We therefore calculate their production rates at the LHC. To do this, first we calculate exactly the effective Lagrangian containing KK number violating operators. Through the KK number violation operator, $\gamma^{(2)}$ and $Z^{(2)}$ decay into dilepton. In addition to the decay mode, single second KK particle production can be allowed, which does not suffer from a severe kinematical suppression compared to pair productions. Next we study the production processes of $\gamma^{(2)}$ and $Z^{(2)}$ including both the KK number violating and conserving processes. At the LHC, $\gamma^{(2)}$ and $Z^{(2)}$ are produced mainly through the cascade decays of the second KK gluons $g^{(2)}$ and quarks $q^{(2)}$. Here the symbol q stands for both $SU(2)$ doublet and singlet quarks. We also need to calculate their branching ratios into $\gamma^{(2)}$ and $Z^{(2)}$. Finally, we calculate the production rates of $\gamma^{(2)}$ and $Z^{(2)}$ from each process, and estimate the number of the dilepton signals from them.

This article is organized as follows. In the next section, we briefly review the MUED model. Then we mention the difficulty that appears during the confirmation of the MUED model at the LHC, and discuss an idea to overcome the difficulty. In Sec. 3, we discuss the Lagrangian relevant to the productions of $\gamma^{(2)}$ and $Z^{(2)}$, and we calculate the branching ratios of colored second KK particles. In Sec. 4, we show some numerical results for $\gamma^{(2)}$ and $Z^{(2)}$ productions, and discuss the significance to discover the particles at the LHC. Section 5 is devoted to summary.

2 The MUED model and its discrimination from other models

The MUED model is the simplest version of the UED models. In this model, fields with a fifth dimensional momentum n/R behave as new heavy particles with a tree-level mass $\sqrt{m_{SM}^2 + (n/R)^2}$ from the viewpoint of four dimensional field theory. These new particles are called KK particles, n is called the KK number ($n = 0$ for SM particles, $n = 1, 2, \dots$ for KK particles), and m_{SM} represents the mass of the corresponding SM particle.

The SM particles and their KK particles have identical gauge charges and spins. All interactions of the KK particles in the four dimensional space-time are determined by the Lagrangian in five dimensions. Since the UED models are not renormalizable,

they should be considered as an effective theory defined at the scale Λ , where Λ is usually taken to be $\Lambda R \sim \mathcal{O}(10)$ [1, 9]. In this article, we take Λ to be $\Lambda R = 20^2$. Thus, in order to discuss the phenomenology of the MUED model, we need only two new parameters : $1/R$ and Λ .

Although the masses of KK particles at tree-level are highly degenerate in each KK mode, the degeneracy is slightly relaxed by radiative corrections [10]. The mass spectrum of the n -th KK particles with the radiative corrections δm_n are given by $m_n = \sqrt{(n/R)^2 + m_{SM}^2 + \delta m_n^2}$. Here, analytical expressions of the radiative corrections δm_n are given in Ref. [10]. In general, due to the radiative corrections, colored KK particles are heavier than non-colored KK particles in each KK level. We have used couplings improved by the renormalization group equation to compute the radiative corrections to the masses of KK particles. The mass spectrum of the first KK particles ($n = 1$) and the second KK particles ($n = 2$) for $1/R = 500$ GeV are shown in Table 1. It is seen that each KK mode are degenerate with each other and the masses of the second KK particles are almost twice of the first KK particles.

KK particle	$n = 1$	$n = 2$
KK gluon $g^{(n)}$	618 GeV	1170 GeV
KK Z boson $Z^{(n)}$	536 GeV	1047 GeV
KK W boson $W^{\pm(n)}$	534 GeV	1046 GeV
KK photon $\gamma^{(n)}$	499 GeV	999 GeV
KK Higgs $H^{(n)}$	518 GeV	1014 GeV
KK CP-odd Higgs $A^{(n)}$	512 GeV	1011 GeV
KK charged Higgs $H^{\pm(n)}$	510 GeV	1010 GeV
KK $SU(2)$ singlet electron $E^{(n)}$	505 GeV	1008 GeV
KK $SU(2)$ doublet lepton $L^{(n)}$	514 GeV	1022 GeV
KK $SU(2)$ singlet up quark $U^{(n)}$	571 GeV	1100 GeV
KK $SU(2)$ singlet down quark $D^{(n)}$	569 GeV	1097 GeV
KK $SU(2)$ doublet quark $Q^{(n)}$	582 GeV	1117 GeV
KK light top quark $T^{(n)}$	569 GeV	1071 GeV
KK heavy top quark $t^{(n)}$	594 GeV	1109 GeV
KK $SU(2)$ singlet bottom quark $B^{(n)}$	569 GeV	1097 GeV
KK $SU(2)$ doublet bottom quark $b^{(n)}$	575 GeV	1106 GeV

Table 1: Mass spectrum of KK particles for $1/R = 500$ GeV and $\Lambda R = 20$.

²Our results are almost independent of Λ , since it always appears with a loop suppression and gives only logarithmic corrections.

Since the translational invariance along the extra dimension direction is broken due to the orbifolding on an S^1/Z_2 , the fifth dimensional momentum (KK number) is no longer conserved. Nevertheless, the subgroup of the translational invariance remains unbroken, which is called the KK parity. Under the parity, particles with even (odd) KK number have plus (minus) sign, and the product of the sign is conserved in each process. Because of the KK parity conservation, the lightest KK particle (LKP) is stable and provided as a candidate for dark matter. The situation is quite similar to the case of supersymmetric models with R-parity conservation, in which the Lightest Supersymmetric Particle (LSP) is stable. The relic abundance of the KK particle dark matter has been calculated in the MUED model [7], and it turns out that if the KK particle dark matter dominates the component of dark matter in the universe, $1/R$ should be in the range of 500 GeV-1500 GeV. The MUED model, therefore, would be explored at the LHC.

The confirmation of the MUED model at the LHC is not so easy. Although it is necessary to discover the KK particles, it is very hard to distinguish the signals of these particles from those of other TeV scale models (for example, the MSSM, the little Higgs models, and so on), because these models also predict new heavy particles which give quite similar signals. For example, in a supersymmetric model, new particles also have identical couplings to their corresponding SM particles and the masses of colored new particles are heavier than those of other new particles. Furthermore, there is a conserved discrete symmetry (R parity), which makes LSP stable. In both models, at the LHC, heavy colored new particles are produced first. Then they immediately decay into lighter new particles. Finally the lightest new particles leave detectors as missing energy. The spin difference may be used to discriminate the MUED model from other models [11]. However, the spin determination, particularly when the masses of new particles are degenerate, is difficult at the LHC, and hence the discrimination of TeV scale models is also difficult.

In order to discriminate the signals of the MUED model from those of other models, we focus on the existence of the KK tower. First of all, we need to speculate the value of $1/R$. At the LHC, we can find the signals of first KK particles through the four lepton channel [12]. Through the observations of cascade decays of the first KK particles, we can speculate the value of $1/R$. It is then possible to predict the masses of the second KK particles. The discovery of new particles with predicted masses strongly suggests that the MUED model is realized as new physics at the TeV scale. At tree level, the second KK particles decay into lighter KK particles through KK number conserving processes, and eventually LKPs are left. Since the LKP gives no signal at the detectors, it is very hard to measure the mass of its parent particle. Fortunately, the second KK gauge bosons directly couple with SM fermion

pairs through KK number violating interactions. Consequently, $\gamma^{(2)}$ and $Z^{(2)}$ decay into two charged leptons with nonzero branching ratios, and the masses of $\gamma^{(2)}$ and $Z^{(2)}$ can be clearly reconstructed from the dileptons [8]. The mass difference between $\gamma^{(2)}$ and $Z^{(2)}$ is about 50 GeV for $1/R = 500$ GeV, as shown in Table 1, and for this mass difference each resonance can be distinguished clearly by the observation of dielectron signals [8]. The double peak resonance also suggests the existence of the MUED model, because this is one of the typical signatures of this model. For the discussion of the feasibility to confirm the MUED model at the LHC, we need to know the event rate of the dilepton signals. We thus calculate the production rates of $\gamma^{(2)}$ and $Z^{(2)}$ at the LHC in the following sections.

3 Productions of $\gamma^{(2)}$ and $Z^{(2)}$

In this section, we discuss the Lagrangian relevant to the productions of $\gamma^{(2)}$ and $Z^{(2)}$ bosons. With the Lagrangian we calculate the branching ratios of $g^{(2)}$ and $q^{(2)}$, which are necessary for the discussion of the indirect production of $\gamma^{(2)}$ and $Z^{(2)}$.

3.1 Lagrangian for $\gamma^{(2)}$ and $Z^{(2)}$ productions

First, we show the Lagrangian conserving the KK number relevant to gauge bosons,

$$\begin{aligned}
\mathcal{L}_{\text{con}} = & -g_i \sum_{n=1}^{\infty} \left[\bar{f}^{(n)} t^a \gamma^\mu f^{(n)} V_{i\mu}^{(0)a} \right. \\
& \left. + \bar{f}^{(n)} t^a \gamma^\mu P_{L(R)} f^{(0)} V_{i\mu}^{(n)a} + \bar{f}^{(0)} t^a \gamma^\mu P_{L(R)} f^{(n)} V_{i\mu}^{(n)a} \right] \\
& - \frac{g_i}{\sqrt{2}} \sum_{n,m=1}^{\infty} \left[\bar{f}^{(n)} t^a \gamma^\mu \gamma^5 f^{(m)} V_{i\mu}^{(n+m)a} \right. \\
& \left. + \bar{f}^{(n+m)} t^a \gamma^\mu f^{(n)} V_{i\mu}^{(m)a} + \bar{f}^{(n)} t^a \gamma^\mu f^{(n+m)} V_{i\mu}^{(m)a} \right] \\
& + g_i f_i^{abc} \sum_{n=1}^{\infty} \left[(\partial_\mu V_{i\nu}^{(0)a}) V_i^{(n)b\mu} V_i^{(n)c\nu} \right. \\
& \left. + (\partial_\mu V_{i\nu}^{(n)a}) V_i^{(n)b\mu} V_i^{(0)c\nu} + (\partial_\mu V_{i\nu}^{(n)a}) V_i^{(0)b\mu} V_i^{(n)c\nu} \right], \tag{1}
\end{aligned}$$

where the summation over i , a , b , and c are implicitly made. $f^{(n)}$, g_i , t^a , and $V_{i\mu}^a$ are listed in Table 2. In the third part of the Lagrangian, f_i^{abc} is the structure constant of $SU(3)$ for gluon and that of $SU(2)$ for W boson. As long as we use the KK number conserving Lagrangian, second KK particles are produced in pair due to the KK

n-th KK fermion $f^{(n)}$	g_i	t^a	$V_{i\mu}^a$
$SU(2)$ -singlet charged lepton $E^{(n)}$	$-g'$	1	B_μ
$SU(2)$ -doublet lepton $L^{(n)}$	$-(1/2)g'$	1	B_μ
	g_2	$\sigma^a/2$	W_μ^a
$SU(2)$ -singlet up-type quark $U^{(n)}$	$(2/3)g'$	1	B_μ
	g_s	$\lambda^a/2$	g_μ^a
$SU(2)$ -singlet down-type quark $D^{(n)}$	$-(1/3)g'$	1	B_μ
	g_s	$\lambda^a/2$	g_μ^a
$SU(2)$ -doublet quark $Q^{(n)}$	$(1/6)g'$	1	B_μ
	g_2	$\sigma^a/2$	W_μ^a
	g_s	$\lambda^a/2$	g_μ^a

Table 2: $f^{(n)}$, g_i , t^a , and $V_{i\mu}^a$ in the KK number conserving Lagrangian. B , W , g are $U(1)$, $SU(2)$, $SU(3)$ gauge bosons, g' , g_2 , g_s are $U(1)$, $SU(2)$, $SU(3)$ gauge coupling constants, and σ^a , λ^a are Pauli matrices, Gell-Mann matrices respectively.

number conservation, and hence the production rates are suppressed due to their small phase spaces.

Next we discuss the KK number violating interactions. The effective Lagrangian for the KK number violating operators turns out to be :

$$\mathcal{L}_{\text{vio}} = \frac{x_i}{4} \left\{ N_i(f)c_t + \left[9C_j(f) - \frac{23}{3}C_j(G)\delta_{ij} + \frac{n_j}{3}\delta_{ij} \right] c_j \right\} \bar{f}^{(0)} t_i^a \gamma^\mu P_{L(R)} f^{(0)} V_{i\mu}^{(2)a} , \quad (2)$$

$$c_j \equiv \frac{\sqrt{2}x_j^2}{16\pi^2} \log \frac{\Lambda^2}{\mu^2} , \quad c_t \equiv \frac{\sqrt{2}y_t^2}{16\pi^2} \log \frac{\Lambda^2}{\mu^2} . \quad (3)$$

Here, y_t is the top Yukawa coupling constant, x_i , n_i , $C_i(f)$, $C_i(G)$, and t_i^a are listed in Table 3, and $N_i(f)$ is listed in Table 4. Indices i , and j run over the SM gauge interactions $U(1)$, $SU(2)$, and $SU(3)$, and summation over f is implicitly made. The renormalization scale is denoted by μ . Contribution $9C_j(f)$ comes from Fig. 1 (a), (b), and (c), contribution $-(23/3)C_j(G)\delta_{ij}$ comes from Fig. 1 (d), (e), and (f), and contribution $(n_j/3)\delta_{ij}$ comes from Fig. 1 (g), and (h). Contribution $N_i(f)c_t$ comes from diagrams in Fig. 2.

3.2 Production processes of $\gamma^{(2)}$ and $Z^{(2)}$

We are now in a position to discuss the production processes of $\gamma^{(2)}$ and $Z^{(2)}$. At the LHC, $\gamma^{(2)}$ and $Z^{(2)}$ are produced through two type of processes : (1) direct

	$U(1)$	$SU(2)$	$SU(3)$
x_i	$g'Y_f$	g_2	g_s
n_i	1	2	0
$C_j(f)$	Y_f^2	3/4	4/3
$C_i(G)$	0	2	3
t_i^a	1	$\sigma^a/2$	$\lambda^a/2$

Table 3: Coefficient in the KK number violating operator in the effective Lagrangian (Eq. (2)). g' , g_2 , g_s are $U(1)$, $SU(2)$, $SU(3)$ gauge coupling constants, and Y_f is $U(1)$ hypercharge. σ^a , λ^a are Pauli and Gell-Mann matrices, respectively.

	$Q_3^{(0)}Q_3^{(0)}\gamma^{(2)}, Q_3^{(0)}Q_3^{(0)}W^{(2)}, Q_3^{(0)}Q_3^{(0)}g^{(2)}, T^{(0)}T^{(0)}g^{(2)}$	$T^{(0)}T^{(0)}\gamma^{(2)}$	other
$N(f)$	1	5	0

Table 4: Coefficient $N(f)$ in the KK number violating operator in the effective Lagrangian (Eq. (2)). Q_3 is the third generation $SU(2)$ -doublet quark, and T is $SU(2)$ singlet top quark.

productions and (2) indirect productions via the cascade decays of the second KK colored particles. The production cross sections of $\gamma^{(2)}$ and $Z^{(2)}$ has originally been calculated in Ref. [8], and their calculation includes all of the KK number conserving processes and the direct 1-body production processes of the second KK gauge bosons. In this article, we calculate the production cross sections of $\gamma^{(2)}$ and $Z^{(2)}$ including all significant processes. For example, our calculation includes $pp \rightarrow q^{(2)}q^{(0)}$, $pp \rightarrow \gamma^{(2)}q^{(0)}$, $pp \rightarrow q^{(2)}\bar{q}^{(0)}$ and so on. Importantly, these processes provide large contributions to $\gamma^{(2)}$ and $Z^{(2)}$ productions, particularly for large $1/R$ ($\gtrsim 800$ GeV). We show the relevant processes to the $\gamma^{(2)}$ production in Figs. 3 - 8.

Figure 3 (Fig. 6) shows the direct production of $\gamma^{(2)}$ through KK number conserving (violating) processes. Some of these processes also produce $q^{(2)}$, $\bar{q}^{(2)}$ and $g^{(2)}$, and they decay into $\gamma^{(2)}$ and $Z^{(2)}$. We must include those contributions in the calculation of the production cross section of $\gamma^{(2)}$ and $Z^{(2)}$. Figure 4 (Fig. 7) shows the production of $q^{(2)}$ and $\bar{q}^{(2)}$ through KK number conserving (violating) processes, and Fig. 5 (Fig. 8) shows the production of $g^{(2)}$ through KK number conserving (violating) processes. These colored particles decay into $\gamma^{(2)}$ and $Z^{(2)}$. Here the gray circle in Figs. 6 - 8 stands for the KK number violating vertex. In the s-channel processes in Fig. 7, the contributions from $g^{(2)}$ 1-body direct production are included, while the contributions from $\gamma^{(2)}$ 1-body direct production are not included. Hence,

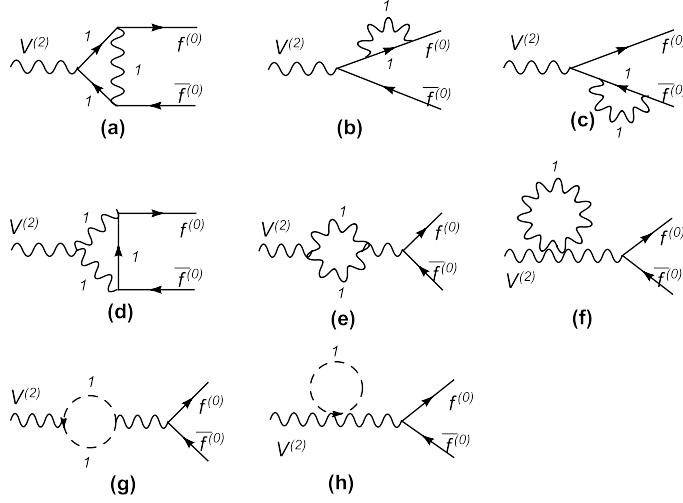


Figure 1: The KK number violating vertices for $\bar{f}^{(0)} t^a \gamma^\mu P_{L(R)} f^{(0)} V_{i\mu}^{(2)a}$ induced from gauge interactions. Attached number represents the KK number of a KK particle in the loop.

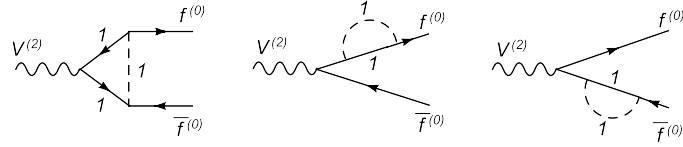


Figure 2: The KK number violating vertices for $\bar{f}^{(0)} t^a \gamma^\mu P_{L(R)} f^{(0)} V_{i\mu}^{(2)a}$ induced from Yukawa interactions. Attached number represents the KK number of a KK particle in the loop.

$\gamma^{(2)}$ 1-body direct production is shown in Fig. 6, and $g^{(2)}$ 1-body direct production is not shown in Fig. 8. Note that the $\gamma^{(2)}$ production from the $Z^{(2)}$ decay can be neglected, because the branching ratio $Z^{(2)} \rightarrow L^{(2)} \bar{L}^{(0)} \rightarrow \gamma^{(2)} L^{(0)} \bar{L}^{(0)}$ is small enough. The processes of $Z^{(2)}$ production are almost same as the $\gamma^{(2)}$ production, so we can skip the discussion of the $Z^{(2)}$ production. In Figs. 6 and 8, processes which have the final state $\gamma^{(2)} \gamma^{(0)}$, $\gamma^{(2)} g^{(0)}$, $g^{(2)} \gamma^{(0)}$, or $g^{(2)} g^{(0)}$ are not shown, because in this calculation, $\gamma^{(0)}$ and $g^{(0)}$ in these processes are the origin of the infrared divergences for the 1-body production processes of second KK gauge bosons. The divergences can be removed by the calculation with a complete treatment.

In order to calculate the indirect production cross sections of $\gamma^{(2)}$ and $Z^{(2)}$, we calculate the branching ratio of $g^{(2)}$ and $q^{(2)}$. We show the branching ratio of the $SU(2)$ singlet KK down-type quark $D^{(2)}$ in Fig. 9, the branching ratio of the $SU(2)$ singlet KK up-type quark $U^{(2)}$ in Fig. 10, and the branching ratio of the $SU(2)$

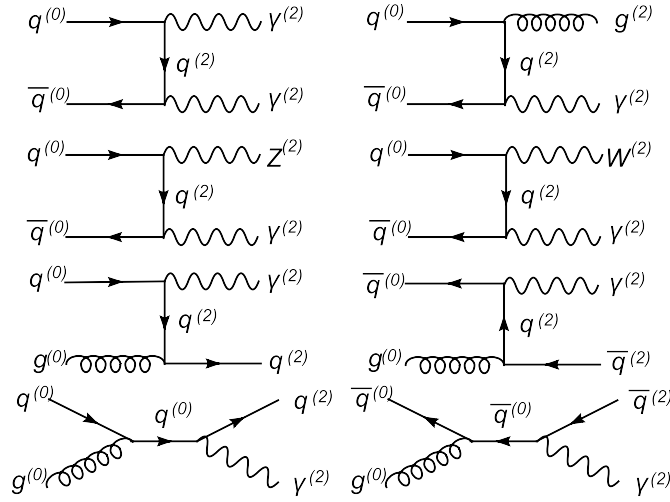


Figure 3: The production of $\gamma^{(2)}$ through KK number conserving processes.

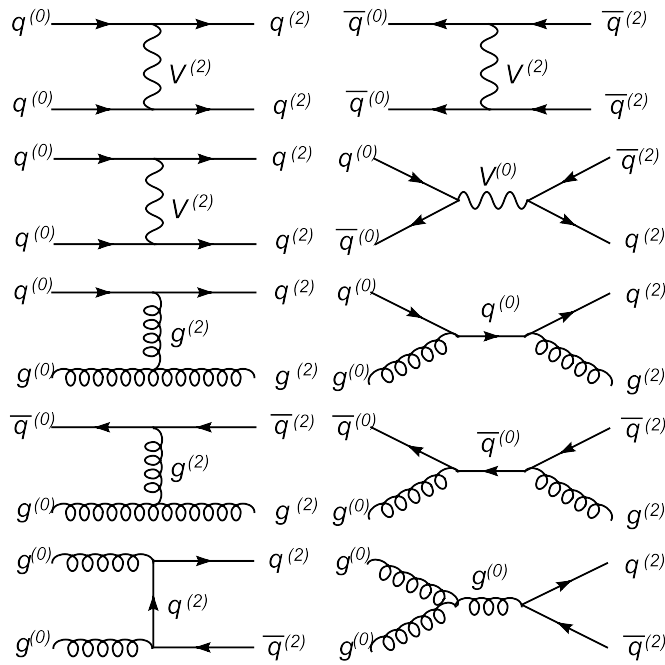


Figure 4: The production of $q^{(2)}$ through KK number conserving processes. V stands for γ , W^\pm , Z , and g .

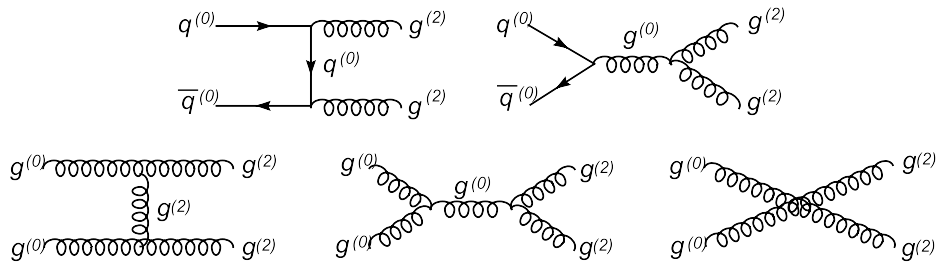


Figure 5: The production of $g^{(2)}$ through KK number conserving processes.

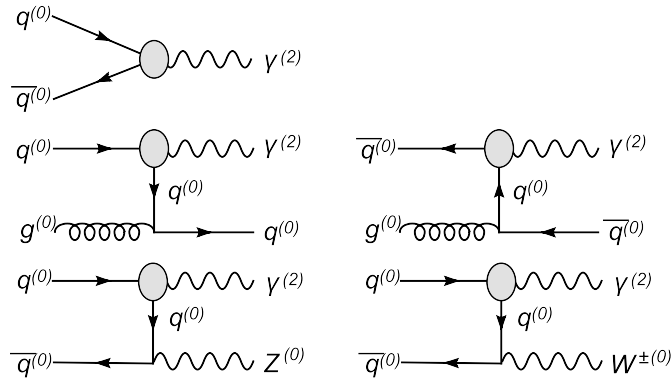


Figure 6: The direct production of $\gamma^{(2)}$ through KK number violating processes. The gray circle represents the KK number violating vertex.

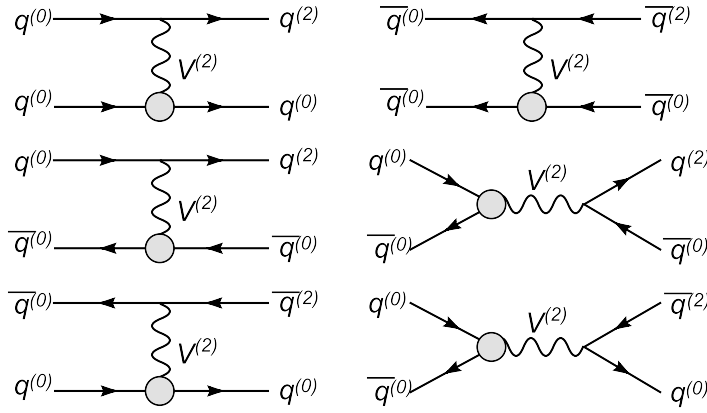


Figure 7: The production of $q^{(2)}$ through KK number violating processes. $V^{(2)}$ stands for $\gamma^{(2)}$, $W^{\pm(2)}$, $Z^{(2)}$, and $g^{(2)}$. The gray circle represents the KK number violating vertex.

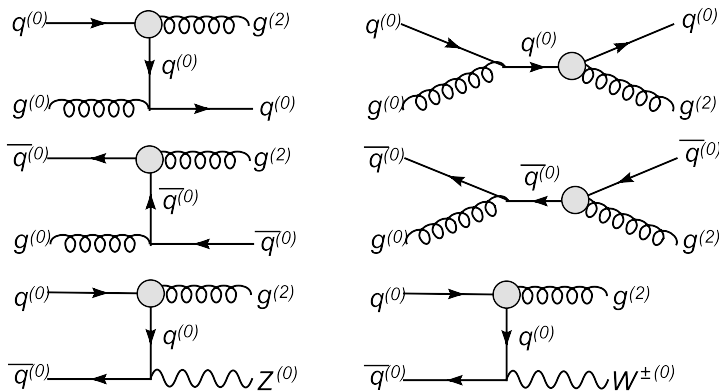


Figure 8: The production of $g^{(2)}$ through KK number violating processes. The gray circle represents the KK number violating vertex.

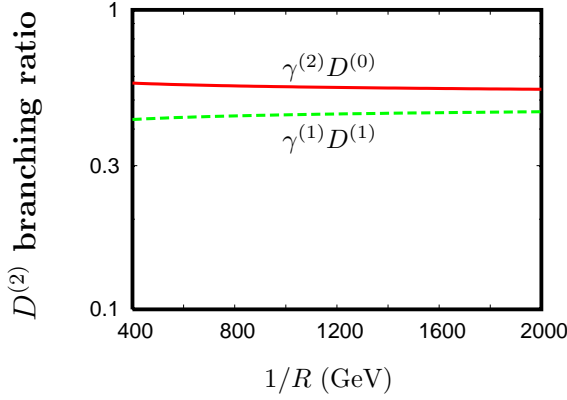


Figure 9: The branching ratio of $D^{(2)}$.

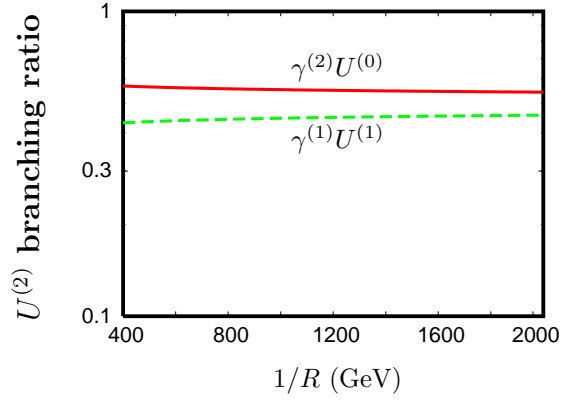


Figure 10: The branching ratio of $U^{(2)}$.

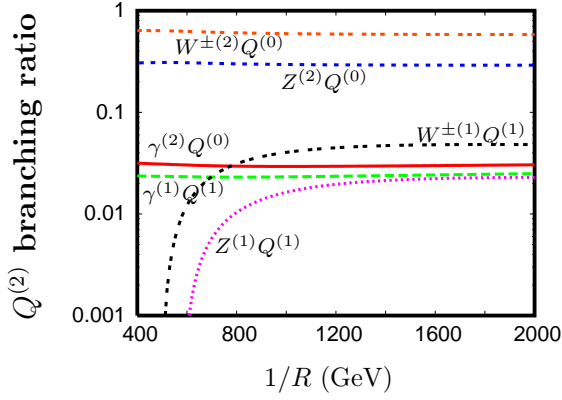


Figure 11: The branching ratio of $Q^{(2)}$.

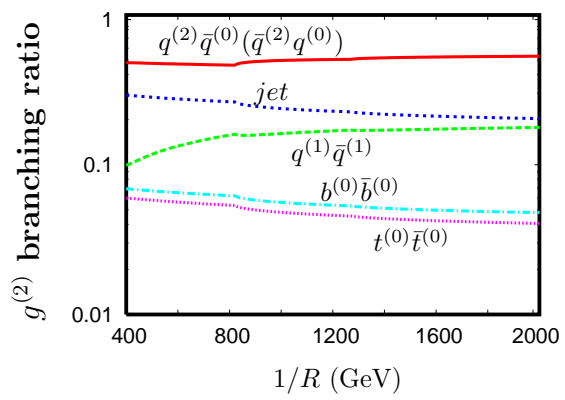


Figure 12: The branching ratio of $g^{(2)}$.

doublet KK quark $Q^{(2)}$ in Fig. 11 as a function of $1/R$. Since $U^{(2)}$ and $D^{(2)}$ are $SU(2)$ singlet, they couple only with the $U(1)$ hypercharge gauge boson. Please note that the Weinberg angle of the neutral KK gauge boson is almost equal to 0 [10], and hence it is possible to identify the KK hypercharge gauge boson as the KK photon. Thus, as shown in Figs. 9 and 10, $D^{(2)}$ and $U^{(2)}$ decay into the KK photon, and $D^{(2)}$ and $U^{(2)}$ can be dominant sources of $\gamma^{(2)}$. On the other hand, $Q^{(2)}$ dominantly decays into $Z^{(2)}$, and hence $Q^{(2)}$ are dominant sources of $Z^{(2)}$.

Finally, we show the branching ratio of $g^{(2)}$ in Fig. 12. In this figure, each line generation indices are implicitly summed, while *jet* represents the sum of first and second generations SM quarks. At the LHC, the production rates of the second KK colored particles are much larger than those of other second KK particles, and $g^{(2)}$ and $q^{(2)}$ dominantly decay into a second KK particle and a SM particle, as shown in these figures. Hence, the indirect productions of $\gamma^{(2)}$ and $Z^{(2)}$ from their cascade decays are quite significant. Note that the branching ratios of each second KK particle calculated in this work are different from that in Ref. [8] due to two reasons. The one

is the difference of the KK number violating operators. In particular, we include the KK number violating operators induced by the top Yukawa coupling. The another one is the difference of a formula of couplings improved by the renormalization group equation to compute the radiative corrections to the masses of KK particles. In the next section, we will calculate the production rates of $\gamma^{(2)}$ and $Z^{(2)}$ using the results in this section.

4 Numerical results

In this section, we present numerical results of the cross sections for $\gamma^{(2)}$ and $Z^{(2)}$ productions and estimate the number of the dilepton signal from $\gamma^{(2)}$ and $Z^{(2)}$ decays at the LHC. The calculations of the cross sections have been performed by using the calcHEP [13] implementing the Lagrangian Eq. (2) derived in the previous section.

In Fig. 13 (Fig. 14), we show the production cross section of $\gamma^{(2)}$ ($Z^{(2)}$) as a function of $1/R$. In the calculation, we have used the CTEQ6L code [14] as a parton distribution function (PDF). Red solid line shows the total cross section of $\gamma^{(2)}$ ($Z^{(2)}$) production. As shown in these figures, for large $1/R$ ($\gtrsim 800$ GeV), the KK number violating processes dominantly contribute to the total production cross section. This means that the KK number violating operators are important for the discrimination of the MUED model from other TeV scale models.

We discuss the significance of each production process. (i) For large $1/R$ ($1/R \gtrsim 800$ GeV), 1-body direct production processes are important, because even if $\gamma^{(2)}$ and $Z^{(2)}$ are too heavy to be produced in pair, these processes provide $\gamma^{(2)}$ and $Z^{(2)}$ efficiently. (ii) In addition to evading the suppression of small phase space, the processes $pp \rightarrow q^{(0)}V^{(2)}(\bar{q}^{(0)}V^{(2)})$ have notable features. Since the PDF of proton is dominated by gluons and the valence quarks, i.e, up- and down-quarks, the rate of $q^{(0)}g^{(0)}$ collision is larger than $q^{(0)}\bar{q}^{(0)}$ collision. Furthermore, the cross section of these processes has the large logarithm factor :

$$\sigma \sim \log \left[\frac{(s - m_{V_2}^2) + m_{q_0}^2}{m_{q_0}^2} \right]. \quad (4)$$

Here m_{q_0} is the mass of a SM quark, m_{V_2} is the mass of second KK gauge boson, and s is the square of the initial state total energy. In usual cases, cross sections decrease according to the increasing of $1/R$ and s . However, this logarithm factor prevents the drastic decreasing. Thus, in all range of $1/R$ in these figures, indirect productions from $pp \rightarrow q^{(0)}g^{(2)}(\bar{q}^{(0)}g^{(2)})$ and direct productions $pp \rightarrow q^{(0)}\gamma^{(2)}(\bar{q}^{(0)}\gamma^{(2)})$ or $pp \rightarrow q^{(0)}Z^{(2)}(\bar{q}^{(0)}Z^{(2)})$ provide contribution of more than 10% to total production cross sections. (iii) At the LHC, the final state $q^{(2)}\bar{q}^{(0)}$ (or $\bar{q}^{(2)}q^{(0)}$) is mostly provided

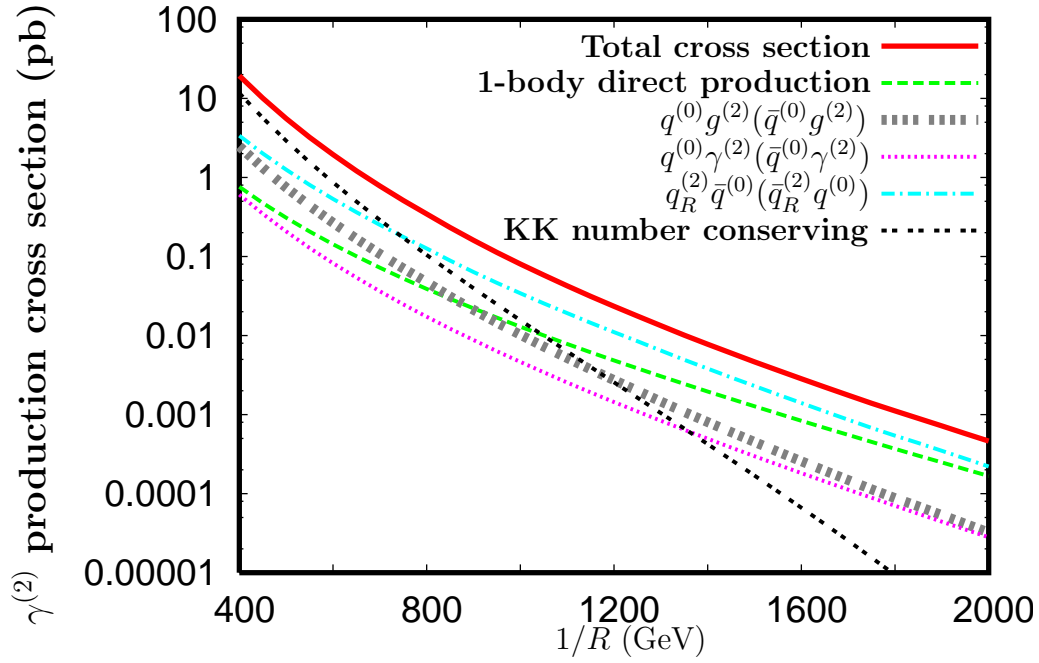


Figure 13: The production cross sections of $\gamma^{(2)}$. Red solid line shows the total cross section, and each line shows partial cross section for each process as denoted in the legend.

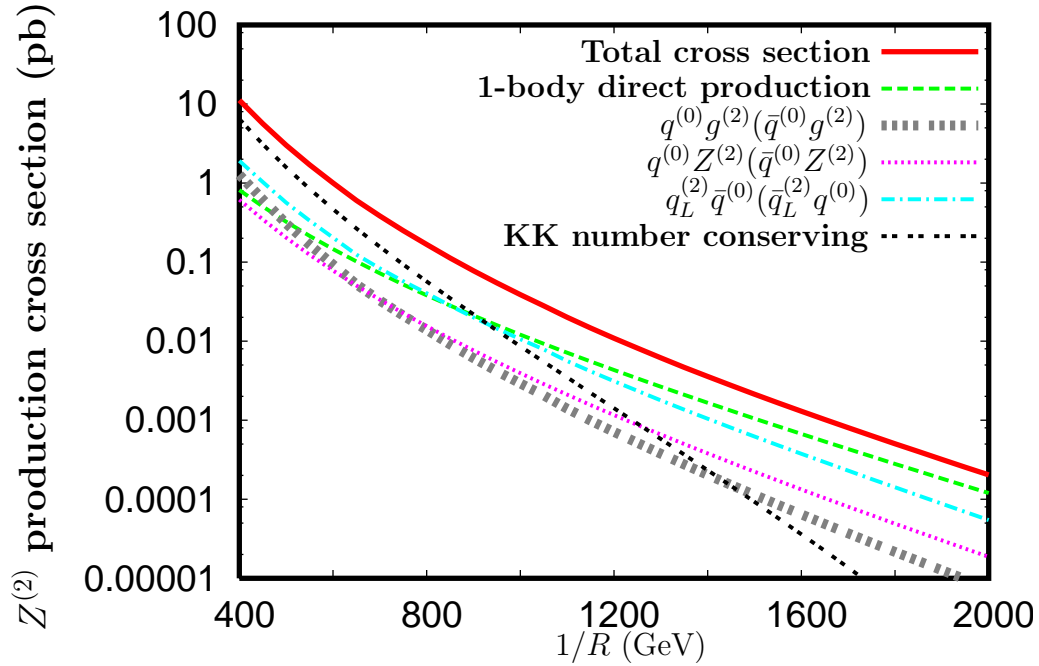


Figure 14: The production cross sections of $Z^{(2)}$. Red solid line shows the total cross section, and each line shows partial cross section for each process as denoted in the legend.

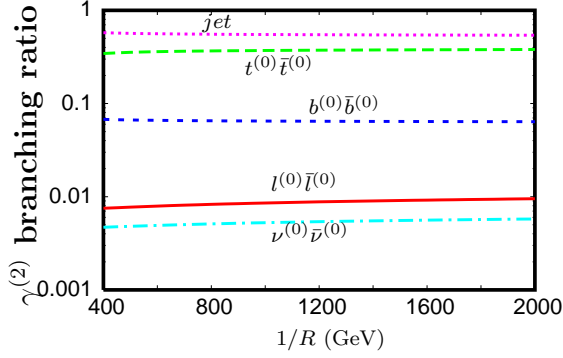


Figure 15: The branching ratio of $\gamma^{(2)}$.

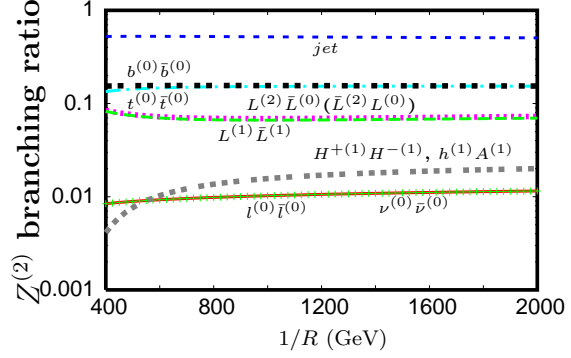


Figure 16: The branching ratio of $Z^{(2)}$.

by the s-channel process mediated by $g^{(2)}$ propagator. In other words, these include the contributions from $g^{(2)}$ 1-body production and indirect productions through the cascade decay of $g^{(2)}$. In this case, the pole resonance of $g^{(2)}$ leads the large enhancement of the cross section. Thus the processes $pp \rightarrow q_{R(L)}^{(2)}\bar{q}^{(0)}$ ($\bar{q}_{R(L)}^{(2)}q^{(0)}$) have large cross sections, even if $1/R$ is rather large, and provide large contributions to the indirect productions of $\gamma^{(2)}$ and $Z^{(2)}$. (iv) For small $1/R$ ($\lesssim 800$ GeV), the cross sections of KK number conserving processes are larger than those of KK number violating processes, because the KK number conserving operators have no loop suppressions. However, for large $1/R$ ($\gtrsim 800$ GeV), the contribution from KK number conserving processes decreases rapidly because of the severe kinematical suppression on the pair production of the second KK particles.

Assuming an integrated luminosity of 100 fb^{-1} , the number of produced $\gamma^{(2)}$ and $Z^{(2)}$ are calculated as $10^6 - 10^2$ for $400 \text{ GeV} \leq 1/R \leq 2000 \text{ GeV}$. Once $\gamma^{(2)}$ and $Z^{(2)}$ are produced, they decay into dileptons with nonzero branching ratios. In order to estimate the number of dilepton signals from $\gamma^{(2)}$ and $Z^{(2)}$, we calculate these branching ratios. Figure 15 (Fig. 16) shows the branching ratio of $\gamma^{(2)}$ ($Z^{(2)}$). In both figures, each line generation indices are implicitly summed. $\gamma^{(2)}$ is the lightest second KK particle, and the masses of the first KK fermions are always heavier than the half of the $\gamma^{(2)}$ mass. Then $\gamma^{(2)}$ must decay into SM fermion pair through KK number violating processes. On the other hand, $Z^{(2)}$ has many decay channels comparing with $\gamma^{(2)}$. Although the decay channels of $\gamma^{(2)}$ and $Z^{(2)}$ are quite different with each other, coincidentally the branching ratio to dilepton is almost the same.

In Table 5, we show the number of the dilepton signals with assuming the luminosity 100 fb^{-1} . Dilepton events are expected to occur at least once for $1/R \lesssim 1600$ GeV. If the MUED model is realized by the nature in addition to the dilepton signals from the decay of $\gamma^{(2)}$ and $Z^{(2)}$, many new particles with degenerate mass

$1/R$	dileptons from $\gamma^{(2)}$	dileptons from $Z^{(2)}$
400 GeV	1.5×10^4	9.4×10^3
800 GeV	2.9×10^2	1.6×10^2
1200 GeV	2.1×10	1.2×10
1600 GeV	2.6	1.4
2000 GeV	4.4×10^{-1}	2.3×10^{-1}

Table 5: The number of the dilepton signals at the LHC with 100 fb^{-1} .

spectrum around $1/R$ (i.e., the first KK particles) are discovered. Connecting the observational results of dilepton signals and the discovery of the first KK particles, it is possible to confirm the MUED model. In this work, we do not discuss the feasibility of the MUED model confirmation, which need a complete analysis with Monte Carlo simulation. It is beyond the scope of this paper. This will be addressed in future work [15].

5 Summary

At the LHC, the discrimination of the MUED model from other models is difficult, because the signals of new particles of TeV scale models are quite similar to each other. For the discrimination, we focused on a distinct feature of the MUED model, i.e., the existence of the KK tower. Once $\gamma^{(2)}$ and $Z^{(2)}$ are produced, they can decay into dilepton which provides a very clear signal of the second KK particles. The discovery of the second KK particles strongly indicates the existence of the KK tower and consequently will lead to the confirmation of the MUED model. In order to estimate the number of the dilepton events from $\gamma^{(2)}$ and $Z^{(2)}$, we have calculated the production rates of $\gamma^{(2)}$ and $Z^{(2)}$ at the LHC.

First we have calculated the KK number violating operators. They play a crucial role, because $\gamma^{(2)}$ and $Z^{(2)}$ can decay into dilepton through these couplings. Next we have shown all significant processes for $\gamma^{(2)}$ and $Z^{(2)}$ productions including both the KK number conserving and violating interactions. Then we have calculated the production cross sections of $\gamma^{(2)}$ and $Z^{(2)}$. Finally we have found that $\mathcal{O}(10^2)$ - $\mathcal{O}(10^6)$ of $\gamma^{(2)}$ and $Z^{(2)}$ production events are expected for $400 \text{ GeV} \leq 1/R \leq 2000 \text{ GeV}$ with an integrated luminosity of 100 fb^{-1} . We have also discussed the significance of various production processes and found that the KK number violating processes give leading contributions to the $\gamma^{(2)}$ and $Z^{(2)}$ productions for $1/R \gtrsim 800 \text{ GeV}$.

The number of dilepton events is expected to be at least one for $1/R \lesssim 1600 \text{ GeV}$

with 100 fb^{-1} integrated luminosity. For the discrimination, it is crucial whether the dilepton signals can be observed or not. We need further study to discuss the feasibility of the discovery of the MUED model by estimating the background from the SM. We leave this for future work [15].

Acknowledgments

The work of J. S. was supported in part by the Grant-in-Aid for the Ministry of Education, Culture, Sports, Science, and Technology, Government of Japan (No. 20025001, 20039001, and 20540251). The work of M. Y. was supported in part by the Grant-in-Aid for the Ministry of Education, Culture, Sports, Science, and Technology, Government of Japan (No. 20007555).

References

- [1] T. Appelquist, H. C. Cheng and B. A. Dobrescu, Phys. Rev. D **64** (2001) 035002.
- [2] I. Antoniadis, Phys. Lett. B **246** (1990) 377.
- [3] H. C. Cheng, J. L. Feng and K. T. Matchev, Phys. Rev. Lett. **89** (2002) 211301; G. Servant and T. M. P. Tait, Nucl. Phys. B **650** (2003) 391.
- [4] B. A. Dobrescu and E. Poppitz, Phys. Rev. Lett. **87** (2001) 031801.
- [5] S. Matsumoto, J. Sato, M. Senami and M. Yamanaka, Phys. Lett. B **647** (2007) 466.
- [6] K. Agashe, N. G. Deshpande and G. H. Wu, Phys. Lett. B **511** (2001) 85; K. Agashe, N. G. Deshpande and G. H. Wu, Phys. Lett. B **514** (2001) 309; T. Appelquist and B. A. Dobrescu, Phys. Lett. B **516** (2001) 85; T. Appelquist and H. U. Yee, Phys. Rev. D **67** (2003) 055002; J. F. Oliver, J. Papavassiliou and A. Santamaria, Phys. Rev. D **67** (2003) 056002; D. Chakraverty, K. Huitu and A. Kundu, Phys. Lett. B **558**, (2003) 173; A. J. Buras, M. Spranger and A. Weiler, Nucl. Phys. B **660**, (2003) 225; P. Colangelo, F. De Fazio, R. Ferrandes and T. N. Pham, Phys. Rev. D **73**, (2006) 115006; I. Gogoladze and C. Macesanu, Phys. Rev. D **74** (2006) 093012.
- [7] M. Kakizaki, S. Matsumoto, Y. Sato and M. Senami, Phys. Rev. D **71** (2005) 123522; S. Matsumoto and M. Senami, Phys. Lett. B **633** (2006) 671; F. Burnell and G. D. Kribs, Phys. Rev. D **73** (2006) 015001; M. Kakizaki, S. Matsumoto and M. Senami, Phys. Rev. D **74** (2006) 023504; K. Kong and K. T. Matchev, JHEP **0601** (2006) 038; S. Matsumoto, J. Sato, M. Senami and M. Yamanaka, Phys. Rev. D **76** (2007) 043528.
- [8] A. Datta, K. Kong and K. T. Matchev, Phys. Rev. D **72** (2005) 096006 [Erratum-ibid. D **72** (2005) 119901].
- [9] G. Bhattacharyya, A. Datta, S. K. Majee and A. Raychaudhuri, Nucl. Phys. B **760** (2007) 117.
- [10] H. C. Cheng, K. T. Matchev and M. Schmaltz, Phys. Rev. D **66** (2002) 036005.
- [11] A. J. Barr, Phys. Lett. B **596** (2004) 205.
- [12] G. H. Brooijmans *et al.*, arXiv:0802.3715 [hep-ph].
- [13] A. Pukhov, arXiv:hep-ph/0412191.
- [14] J. Pumplin, D. R. Stump, J. Huston, H. L. Lai, P. Nadolsky and W. K. Tung, JHEP **0207** (2002) 012.
- [15] S. Matsumoto, J. Sato, M. Senami and M. Yamanaka, work in progress.